ISSN: 1803-3814 (Printed), 2571-3701 (Online)
https://doi.org/10.13164/mendel.2023.1.071

MENDEL Soft Computing Journal

The Routh Hurwitz Criteria for Studying The Stability and Bifurcation in Multispiral Chua Chaotic Attractor

Malika Belouerghi[1], Tidjani Menacer[1,✉], René Lozi[2]

[1]Laboratory of Applied Mathematics, University Mohamed Khider of Biskra, P.O. Box 145, Biskra 07000, Algeria
[2]University Côte d'Azur, CNRS, LJAD, France, Parc Valrose 06108, Nice Cédex 02
m.belouerghi@univ-biskra.dz, m.tidjani@univ-biskra.dz✉, Rene.Lozi@univ-cotedazur.fr

Abstract

This article discusses the multispiral Chua Chaotic attractor's hidden bifurcations that are generated by the sine function. The number of spirals (also known as a multiscroll attractor) that are controlled by the integer parameter c can be used to describe the basic shape of chaotic attractors. Since this parameter is an integer, increasing it by one does not allow the observation of bifurcations from n to $n+2$ spirals. The method of hidden bifurcations, however, enables the observation of such bifurcations by adding a real parameter ε. Chaotic attractors with either an even or an odd number of spirals are visible along the marked paths of bifurcation. Moreover, this additional hidden parameter allows finding the bifurcation of the multispiral Chua attractor from a stable state to a chaotic state. Furthermore, the Routh-Hurwitz criteria are used to study the stability of the original equilibrium point of the Chua attractor.

Keywords: *Bifurcation, Chua's Circuit, Hidden Attractor, Hidden Bifurcation, Stability.*

Received: 17 April 2023
Accepted: 25 June 2023
Online: 30 June 2023
Published: 30 June 2023

1 Introduction

In the framework of the qualitative theory of dynamic systems, the name "bifurcation" was coined by Henri Poincaré in 1885 [24]. For a given value of a parameter, a bifurcation is seen when the number of solutions to a family of differential equations increases from one to two, like the pitchfork of a branch of a tree [25], [18], or when the topological structure of the solution is changed from steady state to periodic function (Hopf bifurcation [21]), or from periodic to quasi-periodic function (secondary Hopf bifurcation).

Lorenz [17], extended the scope of the bifurcation theory by identifying the first chaotic strange attractor in 1963. Chua invented the first differential equation modeling a real electronic device system with a chaotic asymptotic attractor (hence the strange attractor) while he was invited Professor at Matsumoto's laboratory, Waseda University, Tokyo [4].

Nowadays, Chua's attractor is widely used, due to both its realizations: electronic circuit or its mathematical model. The electronic circuit and the system of differential equations may be combined to reach multiple objectives by Duan et al. [7]. One can consider Chua's circuit as the simplest electronic circuit presenting chaos and possessing a highly interesting dynamical behavior. This was checked in many laboratory experiments for Zhong and Ayrom [31], computer simulations for Matsumoto [22] and rigorously done mathematics [5], [19], [3].

Chua's circuit is, surely the most extensively studied chaotic electrical system. It has the extraordinary feature to be able to generate a large variety of dynamical behaviours with just a few self-electronic components. In particular, it consists in two linear capacitors (a resistor and an inductor) and one non-linear resistor known as Chua's diode. By appropriately choosing these components, the circuit becomes chaotic, and the trajectories tend to a limit set called strange attractor. The best-known attractor generated by Chua's circuit is called double scroll [28], [2]. It had been generalized in several ways, replacing continuous piecewise-linear functions with some smooth functions, such as polynomials [10], [26], [9], and [8], etc.

The modified family defined in [27], [30], generates attractors with even or odd number of scrolls. The n-double scrolls correspond to the even case ($2n$-scroll attractors in the new family) with Chua's double scroll being a 2-scroll attractor.

In the work of Tang et al. [29], it is demonstrated that the n-scroll attractors can be generated using a simple sine or a cosine function.

In 2011, Leonov et al. [12], [11] introduced a new classification of attractors of non-linear dynamical systems; in which attractors are dispatched in self-excited or hidden attractors. The first ones can be localized numerically via a standard computational procedure.

After a transient process, a trajectory, starts from a point of unstable manifold in a neighborhood of equilibrium to reach a state of oscillation. Hence, one can easily identify it. In contrast, for hidden attractors, a basin attraction does not intersect with small neighborhoods of equilibria. To localize them, it is necessary to develop special procedures. Therefore, there are no transient processes leading to such attractors. The name hidden comes from this property.

Hidden attractors play a key role in engineering applications (such as air crafts control systems, electrical machines, etc.) as they allow unexpected and potentially catastrophic responses to perturbations in a structure.

An effective method for the numerical localization of hidden attractors in multidimensional dynamical systems has been proposed by the previously cited authors [15], [14]. Their method is based on numerical continuation: a sequence of similar systems is constructed such that for the first (starting) system the initial data for numerical computation of possible oscillating solution (starting oscillation) can be obtained analytically and its transformation from one system to another is followed numerically. One can find the first example of a hidden chaotic strange attractor in Chua's attractor [13].

The modified multispiral Chua system with a sine function is presented in [29]. In [23], Menacer et al. using the Kuznetsov and Leonov method in another way, found a sequence of hidden bifurcations.

In this system, the parameter c governing the number of spirals is an integer; hence it is not possible to vary it continuously. Therefore, it is not possible to observe classical bifurcations of attractors from n to $n+2$ spirals when the parameter c changes, because the theory of bifurcation concerns the variation of solutions with respect to a continuous parameter. Also, it is not possible to use non-integer real values for c. To overcome this obstacle, a new bifurcation parameter ε is introduced by the hidden attractor search method. In this method, the parameter ε controls the birth of an attractor and the increase of the number of spirals until the final number corresponding to the value of the integer c (in this article c is set to 11 and 12) is reached.

In this paper, a second role has been assigned to the parameter ε: the control of the nature of solutions (transition from stability to chaos). The Routh-Hurwitz criterion given in [1] is used for the study of the stability of the origin equilibrium point with respect to the parameter ε for the multispiral chaotic Chua system considered in this paper.

The organization of the paper is as follows. Attractors with multiSpiral in Chua's sine function system are recalled in Section 2. In Section 3, the hidden bifurcations uncovering method is explained. In the chosen example every attractor located along the hidden bifurcation path have an odd number of spirals. In Section 4, one studies of the stability of the origin equilibrium point E_0 with respect to ε using the Routh-Hurwitz Criteria. Some numerical results are presented in Section 5. Finally, in Section 6, a brief conclusion is drawn.

2 Attractors With Multi-Spiral in Chua's Sine Function System

In [8], the use of cellular neural networks with a piecewise-linear output function to create Complex chaotic attractors with n-double scrolls was highlighted. Another simpler mechanism for generating n-scroll attractors was introduced by Tang in [29], using sine or cosine functions. Since then, in the last decades, multi-scroll chaotic attractors generation has been extensively studied due to their promising applications in various real-world chaos-based technologies including secure and digital communications, random bit generation, etc.

The system of differential equations, describing the behavior of Chua's circuits, that we consider in this article is three-dimensional with a combination of piecewise-linear and sinusoidal nonlinearity [4], [29], [6](see Fig. 1)

$$\begin{cases} \dot{x}(t) &= \alpha(y(t) - f(x(t))), \\ \dot{y}(t) &= x(t) - y(t) + z(t), \\ \dot{z}(t) &= -\beta y(t), \end{cases} \tag{1}$$

where $\dot{x}(t) = \frac{dx(t)}{dt}$, $\dot{y}(t) = \frac{dy(t)}{dt}$, $\dot{z}(t) = \frac{dz(t)}{dt}$.

$$f(x(t)) = \begin{cases} \frac{b\pi}{2a}(x(t) - 2ac) & \text{if} \quad x(t) \geq 2ac, \\ -b\sin(\frac{\pi x(t)}{2a} + d) & \text{if} \quad -2ac < x(t) < 2ac, \\ \frac{b\pi}{2a}(x(t) + 2ac) & \text{if} \quad x(t) \leq -2ac, \end{cases} \tag{2}$$

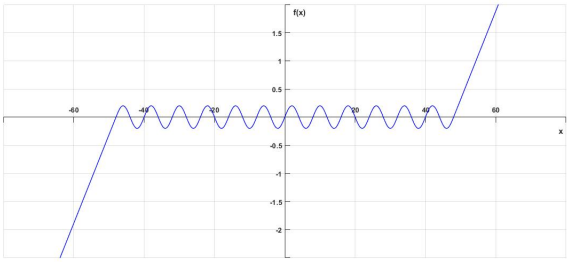

Figure 1: Proposed sine function $f(x)$ with parameters values $a = 2$, $b = 0.2$, $c = 12$, $d = \pi$.

The goal of this article is to analyze the general shape of the attractors and their global geometric features,

which can be described in terms of the number of spirals. In this article the real parameter values have been fixed to $\alpha = 11$, $\beta = 15$, $a = 2$, $b = 0.2$ for which topologically chaotic attractors have been found. They are equivalent to the attractors found in electronic device in [29].

The parameter c is an integer that governs the number n of spirals according to the following formula

$$n = c + 1 \tag{3}$$

and d is chosen such that

$$d = \begin{cases} \pi \text{ if } c \text{ is even.} \\ 0 \text{ if } c \text{ is odd.} \end{cases} \tag{4}$$

A straightforward computation gives the equilibrium points of (1) which are $(-x_{eq}, 0, x_{eq})$ with $x_{eq} = 2ak$, $k = 0, \pm 1, \pm 2, ..., \pm c$ [29]. In the case $c = 12$, one obtains 13 spiral attractors (see Fig. 2). For a complete study of this model with other values of c see [23].

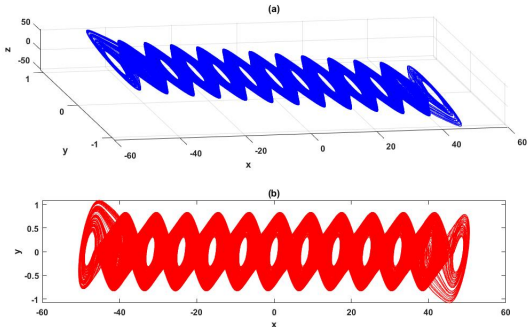

Figure 2: The 13-spiral attractor generated by Equation (1) and (2) for $c = 12$. (a) 3−dimensional figure, (b) Projection into the plane (x, y).

3 Hidden Bifurcations Uncovering Method

Menacer et al. [23] technique for finding hidden bifurcations is based on Leonov and Kuznetsov's fundamental concept for searching hidden attractors (i.e. homotopy and numerical continuation, see Appendix 6). While keeping c constant, a new bifurcation parameter ε is introduced. This method is briefly recalled and applied to (1)-(2) in this section. The value of parameters are fixed to $\alpha = 11$, $\beta = 15$, $a = 2$, $b = 0.2$, $c = 10$, $d = \pi$.

3.1 Hidden Bifurcations

The system(1)-(2) is rewritten in the Lure's form [20]

$$\dot{U} = MU + qH(r^T U), \quad U = (x, y, z) \in \mathbb{R}^3. \tag{5}$$

where

$$M = \begin{pmatrix} 0 & \alpha & 0 \\ 1 & -1 & 1 \\ 0 & -\beta & 0 \end{pmatrix}, \quad q = \begin{pmatrix} -\alpha \\ 0 \\ 0 \end{pmatrix}, \quad r = \begin{pmatrix} 1 \\ 0 \\ 0 \end{pmatrix}$$

and $\mathrm{H}(\sigma)=\mathrm{f}(\sigma)$.

In order to transform system (5) into the form similar to the system (22, see **AppendixA**), a new coefficient χ, and a small parameter ε, are introduced as follows

$$\dot{U} = M_0 U + q\varepsilon g^0(r^T U), \quad U = (x, y, z) \in \mathbb{R}^3. \tag{6}$$

where

$$M_0 = M + \chi q r^T = \begin{pmatrix} -\alpha\chi & \alpha & 0 \\ 1 & -1 & 1 \\ 0 & -\beta & 0 \end{pmatrix},$$

and

$$g(\sigma) = H(\sigma) - \chi\sigma = -\alpha(f(\sigma) - \chi\sigma).$$

Therefore, (6) is written as

$$\begin{cases} \dot{x}(t) &= -\alpha(\chi x(t) - y(t)) + \varepsilon g(x(t)) \\ \dot{y}(t) &= x(t) - y(t) + z(t) \\ \dot{z}(t) &= -\beta y(t) \end{cases} \tag{7}$$

Then considering the transfer function $W(m)$ (21, see **AppendixA**) and solving the equations $\mathrm{Im}\, W(i\omega_0) = 0$ and $\chi = -\mathrm{Re}\, W(i\omega_0)^{-1}$, one obtains $\omega_0 = 2.1018$ and $\chi = 0.03796$.

Using the nonsingular linear transformation $U = SZ$ defined in the **AppendixA**, the system (7) is reduced to the form similar to equation (23)

$$\dot{Z} = AZ + B\varepsilon g^0(C^T Z), \quad Z = (z_1, z_2, z_3) \in \mathbb{R}^3 \tag{8}$$

where

$$A = \begin{pmatrix} 0 & -\omega_0 & 0 \\ -\omega_0 & 0 & 0 \\ 0 & 0 & -d_1 \end{pmatrix}, \quad B = \begin{pmatrix} b_1 \\ b_2 \\ 1 \end{pmatrix}, \quad C = \begin{pmatrix} 1 \\ 0 \\ -h \end{pmatrix}$$

The transfer function $W_A(m)$ of system (8) reads

$$W_A(m) = \frac{-b_1 m + b_2\omega_0}{m^2 + \omega_0^2} + \frac{h}{m + d_1}.$$

Then, using the equality of transfer of both functions $W_A(m)$ and $W_{M_0}(m) = r^T(M_0 - mI)^{-1}q$ to systems (7) and (8) one obtains the following relations

$$\begin{aligned} \chi &= \frac{a + \omega_0^2 - \beta}{\alpha}; \\ d_1 &= \alpha + \omega_0^2 - \beta + 1; \\ h &= \frac{\alpha(\beta - d_1 + d_1^2)}{\omega_0^2 + d_1^2}; \\ b_1 &= \frac{\alpha(\beta - \omega_0^2 - d_1)}{\omega_0^2 + d_1^2}; \\ b_2 &= \frac{\alpha(1 - d_1)(\omega_0 - \beta d_1)}{\omega_0^2(\omega_0^2 + d_1^2)}. \end{aligned}$$

Remark 1. The matrix S is defined by the following relations easily computed

$$A = S^{-1}M_0 S, \quad B = S^{-1}q, \quad C^T = r^T S,$$

$$S = \begin{pmatrix} 1 & 0 & -h \\ \chi & \frac{-\omega_0}{-\alpha} & \frac{hd - h\alpha\chi}{\alpha} \\ \frac{-\beta}{\alpha} & \frac{\chi\beta}{\omega_0} & \frac{\beta h(d - \alpha\chi)}{d\alpha} \end{pmatrix}. \tag{9}$$

3.2 Hidden Bifurcations Route

In this section, we present a numerical example of a hidden bifurcations route. For the values of parameters fixed at the beginning of this section, we obtain

$$\chi = 0.03796, \quad d_1 = 1.4176, \quad h = 26.686,$$

$$b_1 = 15.686, \quad b_2 = 3.1003,$$

therefore, the matrix (9), is

$$S = \begin{pmatrix} 1 & 0 & -26.686 \\ 0.03795 & -0.19107 & -2.4264 \\ -1.3636 & -0.27084 & -25.674 \end{pmatrix}$$

Using *theorem* 1 of the **AppendixA**, for ε small enough, one obtains the initial condition

$$U^0(0) = SZ(0) = S \begin{pmatrix} \tau_0 \\ 0 \\ 0 \end{pmatrix} = \begin{pmatrix} \tau_0 s_{11} \\ \tau_0 s_{21} \\ \tau_0 s_{31} \end{pmatrix}, \qquad (10)$$

Using the notation of Section 2, one obtains for the determination of the initial condition of starting solution for the multistage localization procedure, Chua system

$$x(0) = \tau_0, \quad y(0) = \tau_0 \chi, \quad z(0) = -\tau_0 \frac{\beta}{\alpha}, \qquad (11)$$

Then, the localization procedure described in **Appendix A** is applied to the system (5)-(7). The starting frequency ω_0 and the coefficient of harmonic linearization χ have been already computed in Sec. 3.1. Equation(11), allows to obtain the initial conditions for the first step.

Then, the solutions of system (7) with the nonlinearity $\varepsilon g(x) = \varepsilon(H(x) - \chi x)$ are computed, by increasing sequentially ε from the value $\varepsilon = 0.1$ to $\varepsilon = 1$, with step size 0.1, except between $\varepsilon = 0.9$ and $\varepsilon = 1$, where one uses 0.001 as increasing step. .

All the points of the stable periodic solution $U^1(t)$ corresponding-to $\varepsilon = 0.1$ belong to the domain of attraction of the stable periodic solution $U^2(t)$ corresponding to $\varepsilon = 0.2$. This stable periodic solution $U^2(t)$ is then simply obtained numerically by solving system (5) with $\varepsilon = 0.2$ and $U^1(t_{\max})$ as initial point, where $t_{\max}$ represents the last value of time of integration after discarding the transitory regime. The same numerical procedure is reitered by increasing the ε-value, to obtain the next periodic solutions $U^3(t)$, $U^4(t), ..., U^j(t), ...$ corresponding to the next values of ε. When $\varepsilon = 0.8$ the first chaotic solution one scroll is found.

The initial conditions for recovering the solutions for increasing values of ε as shown in the Table 1.

Table 1: Initials conditions according to the values of ε.

ε	$X^j(0)$	x_0	y_0	z_0
0.1	$U^1(0) = U^0(t_{\max})$	38.3269	-0.0257	-37.9339
0.2	$U^2(0) = U^1(t_{\max})$	-3.7487	0.1619	-5.0818
0.3	$U^3(0) = U^2(t_{\max})$	3.3406	-0.2062	-4.9772
0.4	$U^4(0) = U^3(t_{\max})$	-3.6009	-0.2981	4.7285
0.5	$U^5(0) = U^4(t_{\max})$	3.4797	-0.1484	-5.0577
0.6	$U^6(0) = U^5(t_{\max})$	3.6919	0.0202	-5.1617
0.7	$U^7(0) = U^6(t_{\max})$	4.1512	-0.0232	-5.5316
0.8	$U^8(0) = U^7(t_{\max})$	1.3915	-0.5758	-2.6930
0.86	$U^9(0) = U^8(t_{\max})$	-0.4213	-0.3265	0.2085
0.978	$U^{10}(0) = U^9(t_{\max})$	1.8233	0.2554	-2.6074
0.989	$U^{11}(0) = U^{10}(t_{\max})$	1.4667	0.7801	-0.6740
0.993	$U^{12}(0) = U^{11}(t_{\max})$	3.2919	0.5697	-3.9526
0.995	$U^{13}(0) = U^{12}(t_{\max})$	15.5612	-0.3315	-16.0715
1	$U^{14}(0) = U^{13}(t_{\max})$	-33.7244	-0.0092	35.1636

Using these initial conditions, we get the solutions $U^8(t)$ (Fig. 3(a)) with one spiral to $U^{13}(t)$ (Fig. 4(c)) with 11 spirals. In each figure, there are a different odd number of spirals in the attractor. The number of spirals increases by 2 at each step as displayed in Table 2 from 1 to 11 spirals. The values of ε in this table are exactly the values of bifurcation points with respect to ε. Therefore Fig. 3 and Fig. 4 display the hidden bifurcations of the multi-spiral Chua's attractor.

Table 2: Values of the parameter ε at the bifurcation points for $c = 10$ (11 *spirals*).

ε					
0.80	0.86	0.978	0.989	0.993	0.995
$U^8(0)$	$U^9(0)$	$U^{10}(0)$	$U^{11}(0)$	$U^{12}(0)$	$U^{13}(0)$
1 spiral	3 spirals	5 spirals	7 spirals	9 spirals	11 spirals

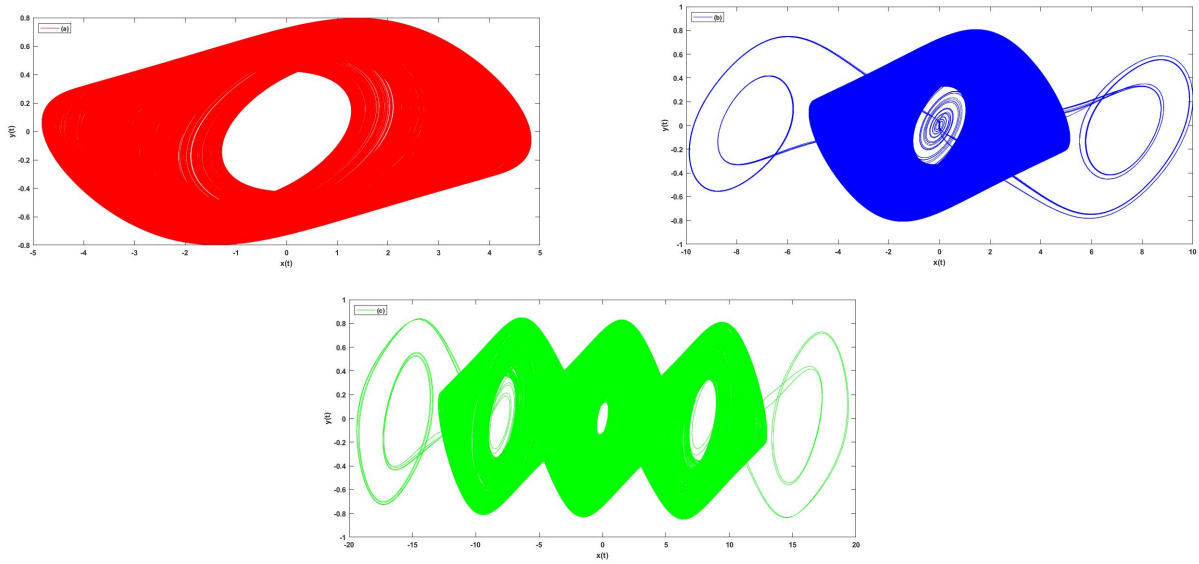

Figure 3: The increasing number of spirals of system (6) with respect to increasing ε values. (a) 1-spiral for $\varepsilon = 0.80$, (b) 3-spirals for $\varepsilon = 0.86$, (c) 5-spirals for $\varepsilon = 0.978$.

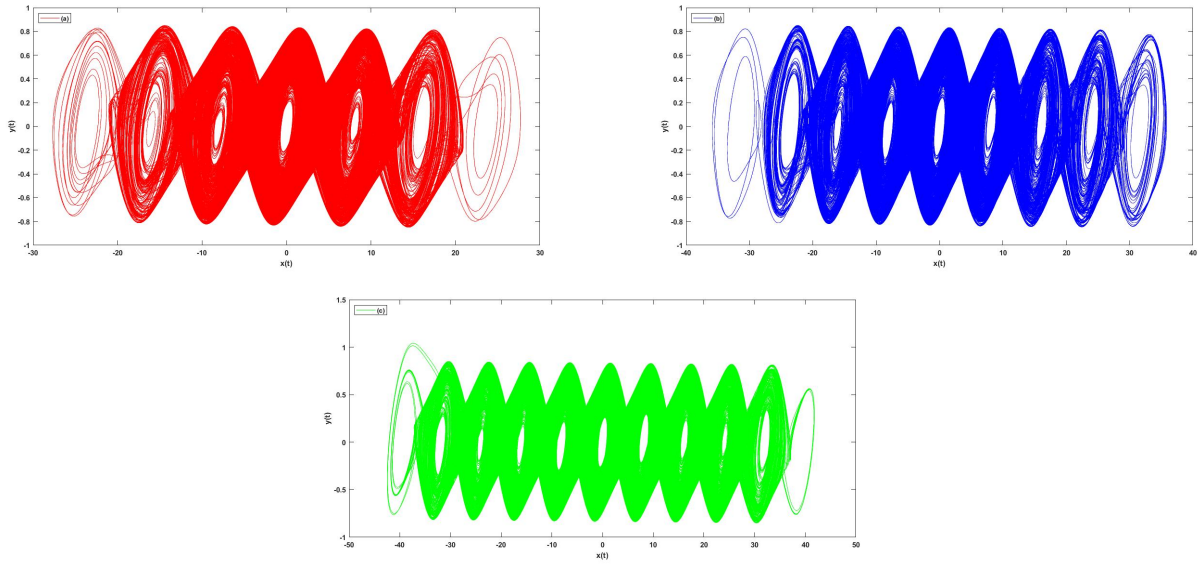

Figure 4: The increasing number of spirals of system (6) with respect to increasing ε values. (a) 7-spirals for $\varepsilon = 0.989$, (b) 9-spirals for $\varepsilon = 0.993$, (c) 11-spirals for $\varepsilon = 0.995$.

4 Stability of the Origin Equilibrium Point E_0 With Respect to ε

In this section, we study the stability of the equilibrium point E_0 with respect to epsilon of the system (7) using Routh-Hurwitz's conditions [1]. In [23] Menacer et al. introduce the concept of hidden bifurcation in the system of Chua adding a new parameter epsilon, which controls the number of spirals. When the value of ε increases from 0 to 1 the number of scrolls decreases. Let $E(x_e, y_e, z_e)$ be an equilibrium solution of the general three-dimensional system:

$$\begin{cases} \dot{x}(t) &= Q(x(t), y(t), z(t)) \\ \dot{y}(t) &= R(x(t), y(t), z(t)) \\ \dot{z}(t) &= V(x(t), y(t), z(t)) \end{cases} \tag{12}$$

The eigenvalues equation corresponding to this equilibrium point is given by the following polynomial:

$$P(\lambda) = \lambda^3 + a_1\lambda^2 + a_2\lambda + a_3. \tag{13}$$

Using the result of the Routh-Hurwitz conditions, where the necessary and sufficient condition for the equilibrium point E to be locally asymptotically stable is $a_1 > 0$, $a_3 > 0$ and $a_1 \times a_2 - a_3 > 0$.

In this section, the parameter c is constant, and the bifurcation is studied with respect to parameter ε, and the values of parameters are $\alpha = 11$, $\beta = 15$, $a = 2$, $b = 0.2$.

4.1 Stability of the Origin Equilibrium Point E_0

The origin $E_0(0, 0, 0)$ is an equilibrium point of System (7) independently to epsilon. In the rest of this article, we consider both cases $c = 11$ with $d = 0$, and $c = 12$ with $d = \pi$.

For $c = 11$ and $d = 0$, the Jacobian matrix for evaluated at the equilibrium point $E_0(0, 0, 0)$ is:

$$\begin{aligned} J_{E_0} &= \begin{pmatrix} -\alpha\chi + \alpha\varepsilon(\chi + \frac{\pi b}{2a}) & \alpha & 0 \\ 1 & -1 & 1 \\ 0 & -\beta & 0 \end{pmatrix} \\ &= \begin{pmatrix} -0.41756 + \varepsilon(0.41756 + \frac{6.908}{4}) & 11 & 0 \\ 1 & -1 & 1 \\ 0 & -15 & 0 \end{pmatrix} \end{aligned}$$

Its characteristic polynomial is:

$$\begin{aligned} P(\lambda) &= \lambda^3 + (1.4176 - 2.1446\varepsilon)\lambda^2 \\ &\quad +(4.4176 - 2.1446\varepsilon)\lambda + (6.2634 - 32.168\varepsilon). \end{aligned}$$

According to Routh-Hurwitz conditions, the necessary and sufficient condition, for the equilibrium point E_0 to be stable is $0.00005139 < \varepsilon < 0.1947$.

Proof.

$$\begin{aligned} a_1 = 1.4176 - 2.1446\varepsilon > 0 &\Longrightarrow \varepsilon < 0.66101; \\ a_3 = 6.2634 - 32.168\varepsilon > 0 &\Longrightarrow \varepsilon < 0.19472; \\ a_1 \times a_2 - a_3 = 4.5993\varepsilon^2 + 19.655\varepsilon - 1.6102 \times 10^{-3} &> 0 \\ \Longrightarrow \varepsilon < -4.2733 \text{ or } \varepsilon > 5.1399 \times 10^{-5}&. \end{aligned}$$

□

For $c = 12$ and $d = \pi$, the Jacobian matrix evaluated at the equilibrium point E_0 is:

$$\begin{aligned} J_{E_0} &= \begin{pmatrix} -\alpha\chi + \alpha\varepsilon(\chi - \frac{\pi b}{2a}) & \alpha & 0 \\ 1 & -1 & 1 \\ 0 & -\beta & 0 \end{pmatrix} \\ &= \begin{pmatrix} -0.41756 + \varepsilon(0.41756 - \frac{6.908}{4}) & 11 & 0 \\ 1 & -1 & 1 \\ 0 & -15 & 0 \end{pmatrix} \end{aligned}$$

Its characteristic polynomial is:

$$\begin{aligned} P(\lambda) &= \lambda^3 + (1.4176 + 1.3094\varepsilon)\lambda^2 \\ &\quad +(1.3094\varepsilon + 4.4176)\lambda + (19.642\varepsilon + 6.2634). \end{aligned}$$

According to Routh-Hurwitz conditions, the equilibrium point E_0 is unstable.

Proof.

$$\begin{aligned} a_1 = 1.4176 + 1.3094\varepsilon > 0 &\Longrightarrow \varepsilon > -1.0826; \\ a_3 = 19.642\varepsilon + 6.2634 > 0 &\Longrightarrow \varepsilon > -0.3188; \\ a_1 \times a_2 - a_3 = 1.7145\varepsilon^2 - 12.001\varepsilon - 1.012 \times 10^{-3} &> 0 \\ \Longrightarrow \varepsilon < -8.4175 \times 10^{-5} \text{ or } \varepsilon > 6.998&. \end{aligned}$$

because there is a contradiction with $0 < \varepsilon < 1$. Therefore, the limit cycle is unstable. □

Special case $\varepsilon = 0$: the system (7) becomes linear:

$$\begin{cases} \dot{x}(t) &= -\alpha\chi x(t) + \alpha y(t) \\ \dot{y}(t) &= x(t) - y(t) + z(t) \\ \dot{z}(t) &= -\beta y(t) \end{cases} \tag{14}$$

The Jacobian matrix is:

$$\begin{aligned} J_{E_0} &= \begin{pmatrix} -\alpha\chi + \alpha\varepsilon(\chi + \frac{\pi b}{2a}) & \alpha & 0 \\ 1 & -1 & 1 \\ 0 & -\beta & 0 \end{pmatrix} \\ &= \begin{pmatrix} -0.41756 + 11\varepsilon(0.03796 + \frac{0.628}{4}) & 11 & 0 \\ 1 & -1 & 1 \\ 0 & -15 & 0 \end{pmatrix}. \end{aligned}$$

The characteristic polynomial is given by:

$$\begin{aligned} P(\lambda) &= \lambda^3 + (1.4176 - 2.1446\varepsilon)\lambda^2 \\ &\quad +(4.4176 - 2.1446\varepsilon)\lambda + (6.2634 - 32.168\varepsilon). \end{aligned}$$

One has

$$\begin{aligned} a_1 = 1.4176 - 2.1446\varepsilon > 0 &\Longrightarrow \varepsilon < 0.66101; \\ a_3 = 6.2634 - 32.168\varepsilon > 0 &\Longrightarrow \varepsilon < 0.19472; \\ a_1 \times a_2 - a_3 = 4.5993\varepsilon^2 + 19.655\varepsilon - 1.6102 \times 10^{-3} &> 0 \\ \Longrightarrow \varepsilon < -4.2733 \text{ or } \varepsilon > 5.1399 \times 10^{-5}&. \end{aligned}$$

Therefore, the Routh-Hurwitz conditions are not verified, because $\varepsilon = 0$, and then the system (7) is unstable. Fig. 5 displays the corresponding unstable limit cycle .

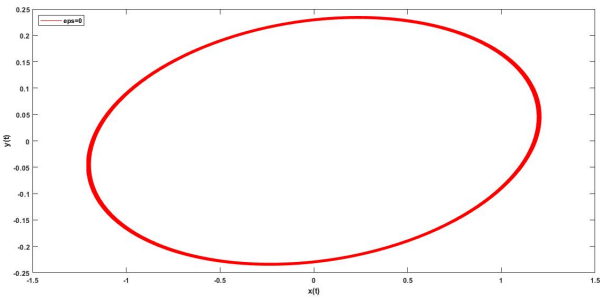

Figure 5: The attractor of the system (7) where $\varepsilon = 0$: limit cycle unstable.

4.2 Other Equilibrium Points

The equilibrium point **E** of system (7) is obtained solving,

$$\begin{cases} \dot{x}(t) = 0 \\ \dot{y}(t) = 0 \\ \dot{z}(t) = 0 \end{cases} \Leftrightarrow \begin{cases} -\alpha(\chi x(t) - y(t)) + \varepsilon g(x(t)) = 0; \\ x(t) - y(t) + z(t) = 0; \\ -\beta y(t) = 0; \end{cases} \tag{15}$$

In addition to the origin equilibrium point $E_0(0,0,0)$, there are several other equilibrium points: $E_{k^+}(x_{eq}, 0, -x_{eq})$ and $E_{k^-}(-x_{eq}, 0, x_{eq})$.

The solution of (15) are :

- If $x \geq 2ac$ or $x \leq -2ac$

$$x_{eq} = \frac{2\varepsilon b\pi ac}{2a(\varepsilon\chi - \chi) - \varepsilon b\pi}.$$

For the values of parameters above, with $c = 11$; one finds:

$$x_{eq} = \pm\frac{27.6460\varepsilon}{0.1518(\varepsilon - 1) - 0.6283\varepsilon}.$$

- If $-2ac < x < 2ac$; one obtains:

$$-\alpha(\chi x(t) - y(t)) + \varepsilon g(x(t)) = 0; \tag{16}$$

that is

$$-\alpha(\chi x(t) - \varepsilon b \sin(\frac{\pi x(t)}{2a}) - \varepsilon\chi x(t)) = 0.$$

Case $\varepsilon = 1$: the system (7) is the original system (1). In this case, in addition to the origin $E_0(0,0,0)$ the other equilibrium points of this system are $(x_{eq}, 0, -x_{eq})$, with $x_{eq} = 2ak$ and $k = \pm1, \pm2, ..., \pm c$ [29].

Case $0 < \varepsilon < 1$: in addition to the origin $E_0(0,0,0)$ the other equilibrium points cannot be obtained using closed formula. It is possible to compute them numerically solving $\dot{x}(t) = 0$ in equation (16). The number of equilibrium points set are shown in Table. 3 and Fig. 6, Fig. 7 replacing the values of parameters above and $c = 11$ in the interval $[-44, 44]$

Table 3: Number of equilibrium points in the equation (16) for different values of ε and $c = 11$.

Values of ε	0.30	0.50	0.70	0.80	0.90	0.95	1
Number of equilibrium points	2	2	6	10	22	22	22

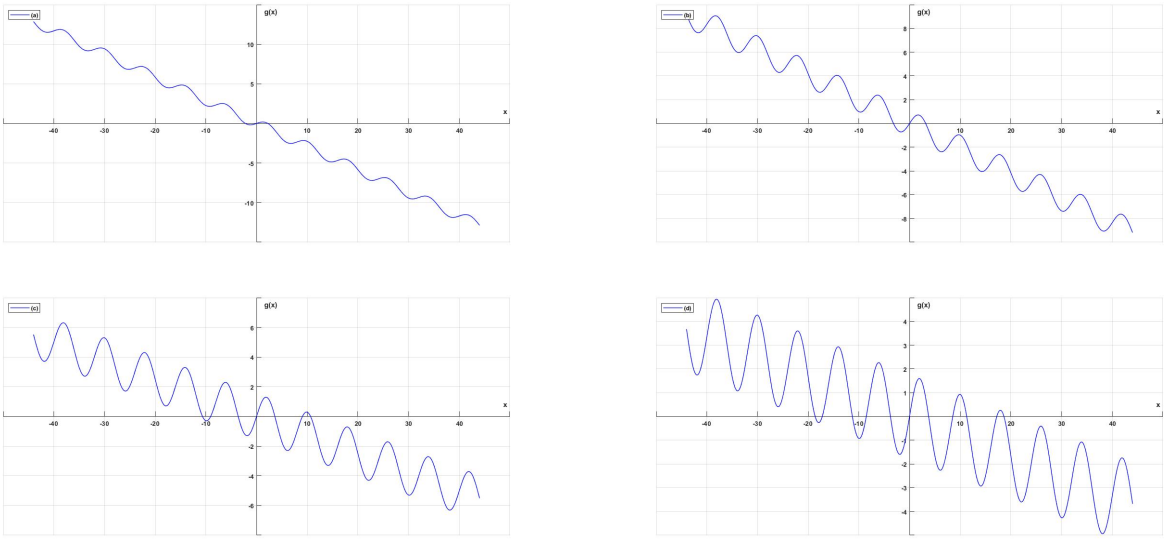

Figure 6: Number of equilibrium points in the equation (16) for different values of ε and $c = 11$. (a) for $\varepsilon = 0.30$, (b) for $\varepsilon = 0.50$, (c) for $\varepsilon = 0.70$, (d) for $\varepsilon = 0.80$.

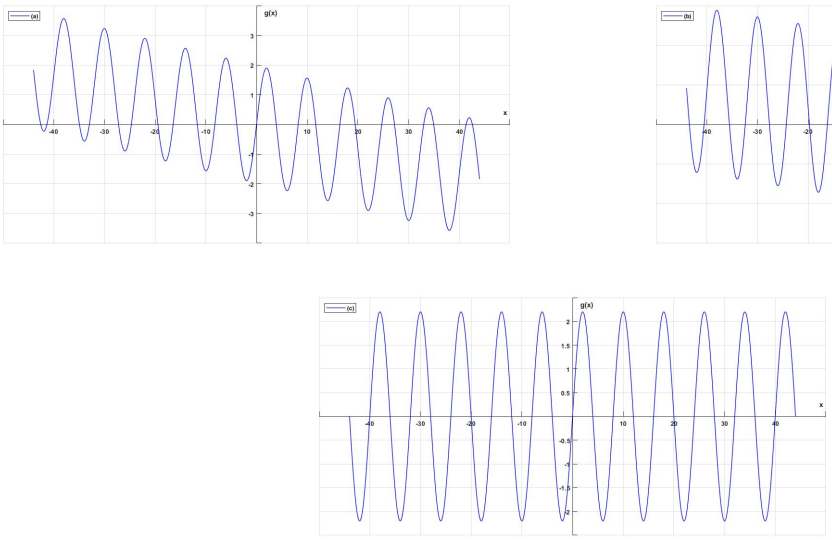

Figure 7: Number of equilibrium points in the equation (16) for different values of ε and $c = 11$. (a) for $\varepsilon = 0.90$, (b) for $\varepsilon = 0.95$, (c) for $\varepsilon = 1$.

5 Numerical Analysis of Bifurcations

5.1 Case $c = 11$

In this section, a numerical analysis of the bifurcations of this system is done for c = 11. In this case one can observe only an even number of scrolls. The value of ε is increased from 0 to 1 . For each value of ε the same initial conditions $[0.001, 0, 0.001]$ are chosen. The bifurcation diagram with respect to ε is given in Fig. 8, Fig. 9 and Fig. 10.

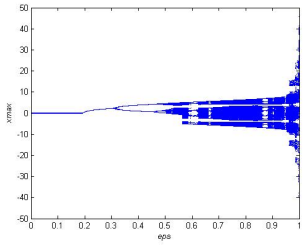

Figure 8: Bifurcation diagram with respect to ε of the component x, with c=11.

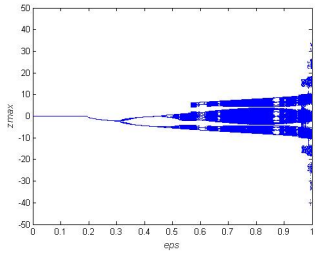

Figure 9: Bifurcation diagram with respect to ε of the component z, with c=11.

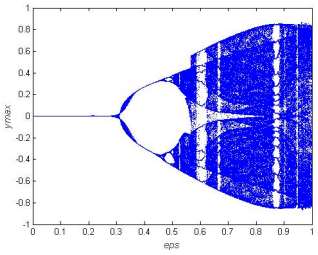

Figure 10: Bifurcation diagram with respect to ε of the component y, with c=11.

In order to highlight the symmetry of the bifurcation diagrams versus the components x and z, Fig. 11 displays the superimposition of both Fig. 8 and Fig. 9.

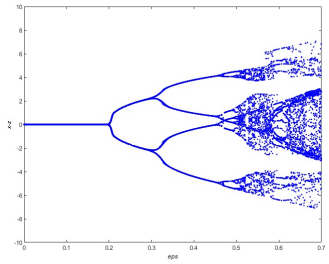

Figure 11: Bifurcation diagram with respect to ε of the superimposed components x and z with c=11.

In Figs. 12 and 13 one displays some corresponding attractors.

- For $\varepsilon < 0.195$, the equilibrium point E_0 is a locally asymptotically stable focus.
- For $0.195 < \varepsilon \leq 0.43$ the fixed point E_0 becomes unstable, a period-one limit cycle appears, as shown in Fig. 12a.
- When $\varepsilon \approx 0.46$, a new bifurcation occurs, the period-one limit cycle becomes unstable and a period-two limit cycle appears (Fig. 12b).
- For $\varepsilon \approx 0.495$, a period-4 limit cycle appears through a new bifurcation, as shown in Fig. 12c, followed by a bifurcation to a period-8 limit cycles at $\varepsilon \approx 0.501$ Fig. 12d). This doubling period bifurcation process continues up to the critical value $\varepsilon = 0.56$, where one chaotic attractor appears (see Fig. 12e). For $\varepsilon = 0.57$ a two-scrolls chaotic attractor appears (see Fig. 12f).

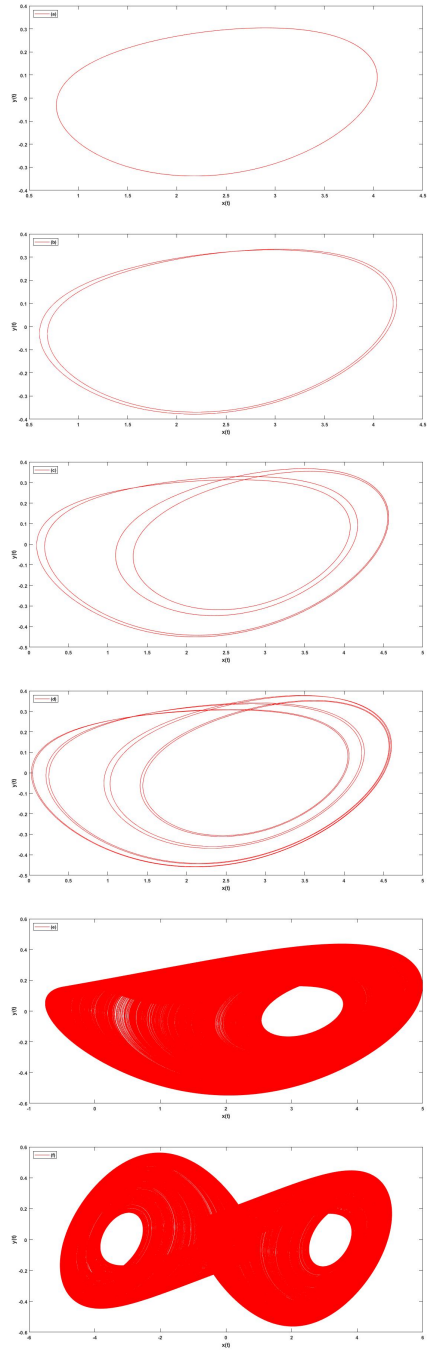

Figure 12: Phase portrait of Chua system for different values ε and $c = 11$(attractors). (a) a period-one limit cycle for $\varepsilon = 0.43$, (b) a period-two limit cycle for $\varepsilon = 0.46$, (c) a period-4 limit cycle for $\varepsilon = 0.495$, (d) a period-8 limit cycle for $\varepsilon = 0.501$, (e) a chaotic attractor chaotic attractor for $\varepsilon = 0.56$, (f) a 2-spirals for $\varepsilon = 0.57$.

Fig. 13 displays the sequence of bifurcations of the number of spirals of the chaotic attractors

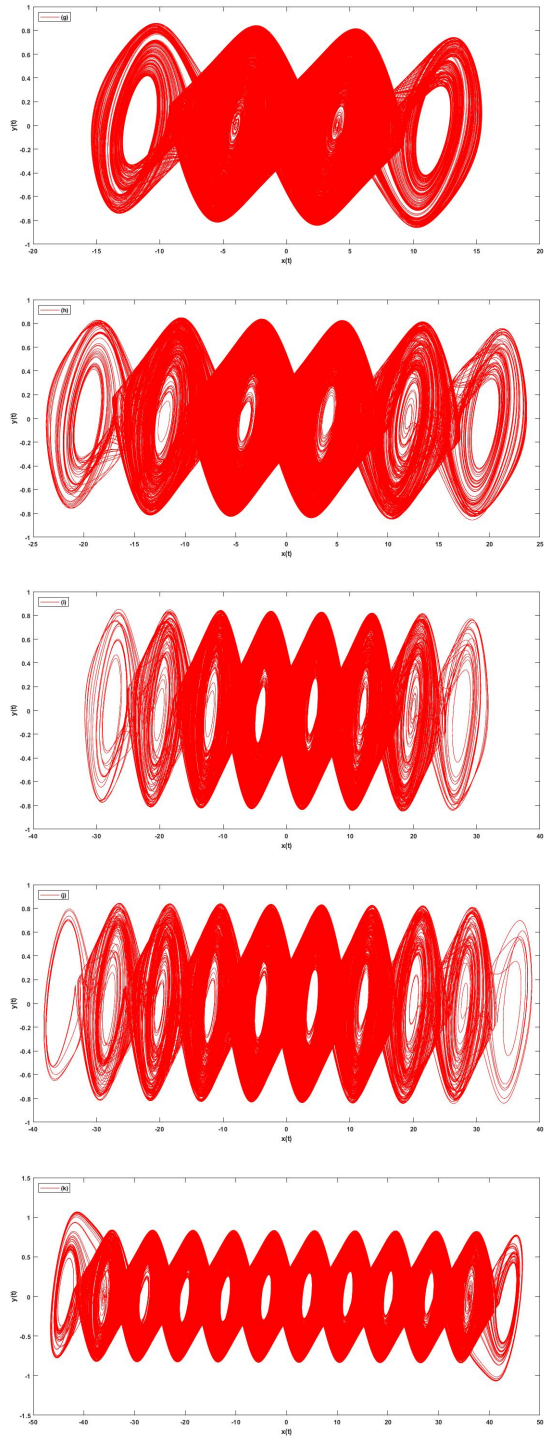

Figure 13: (Continued of Fig. 12). Phase portrait of Chua system for different values ε and $c = 11$(attractors). (g) 4-spirals for $\varepsilon = 0.97$, (h) 6-spirals for $\varepsilon = 0.987$, (i) 8-spirals for $\varepsilon = 0.992$, (j) 10-spirals for $\varepsilon = 0.995$, (k) 12-spirals for $\varepsilon = 0.998$.

5.2 Case $c = 12$

In this case, one can observe only an odd number of scrolls. Fig. 14 displays the bifurcation diagram with respect to ε.

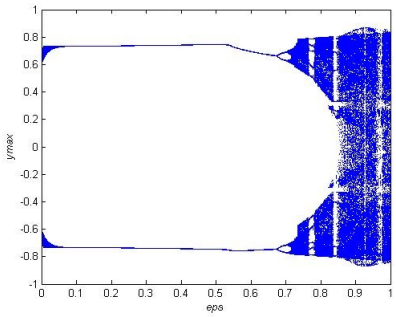

Figure 14: Bifurcation diagram with respect to ε of the component y, for $c = 12$.

In Fig. 15 and 16 one displays some corresponding attractors.

- For $\varepsilon < 0.55$, the equilibrium point E_0 is a locally asymptotically stable focus.
- When $\varepsilon \approx 0.55$, the system of Chua in the fixed point E_0 becomes unstable, and a period-one limit cycle appears for $0.55 < \varepsilon \leq 0.60$, as shown in Fig. 15a.
- When $\varepsilon \approx 0.68$, a new bifurcation occurs, and the period-one limit cycle becomes unstable and a period-two limit cycle appears (Fig. 15b).
- For $\varepsilon \approx 0.706$, a-period-4 limit cycle appears through a new bifurcation, as shown in Fig. 15c, followed by a bifurcation to a period-8 limit cycles at $\varepsilon \approx 0.7109$; (see Fig. 15d). This bifurcation process continues up to a critical value of $\varepsilon = 0.72$, where one chaotic attractor appears; (see Fig. 15e). At $\varepsilon = 0.80$ a 1-scroll chaotic attractor appears (see Fig. 15f).

Fig. 16 displays the sequence of bifurcations of the number of spirals of the chaotic attractors with an odd number of scrolls.

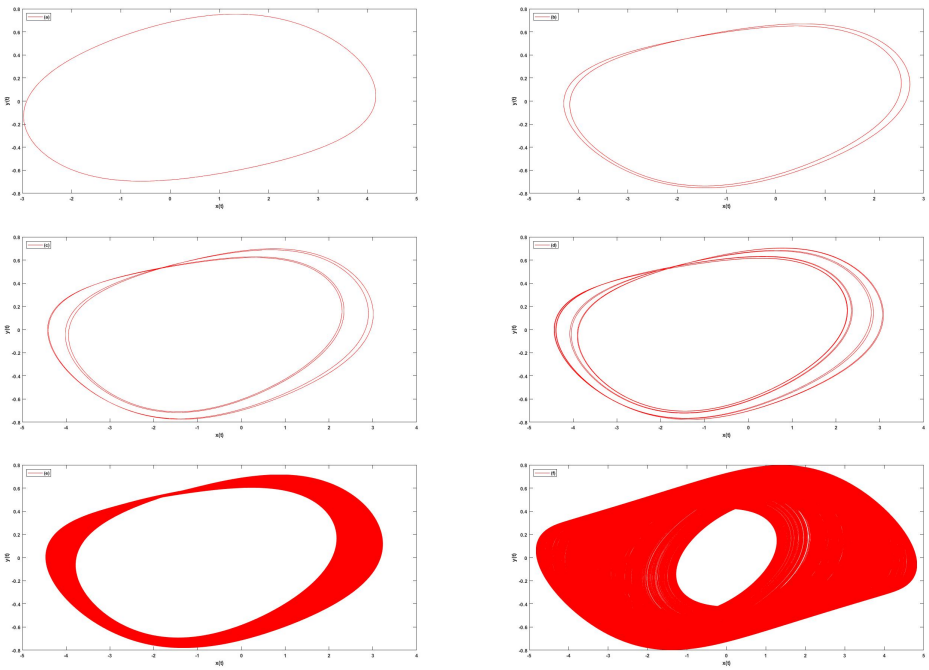

Figure 15: Phase portrait of Chua system for different values ε and $c = 12$(attractors). (a) a limit cycle for $\varepsilon = 0.60$, (b) a period-two limit cycle for $\varepsilon = 0.68$, (c) a period-4 limit cycle for $\varepsilon = 0.706$, (d) a period-8 limit cycle for $\varepsilon = 0.7109$, (e) one chaotic attractor for $\varepsilon = 0.72$, (f) 1-spirals for $\varepsilon = 0.80$

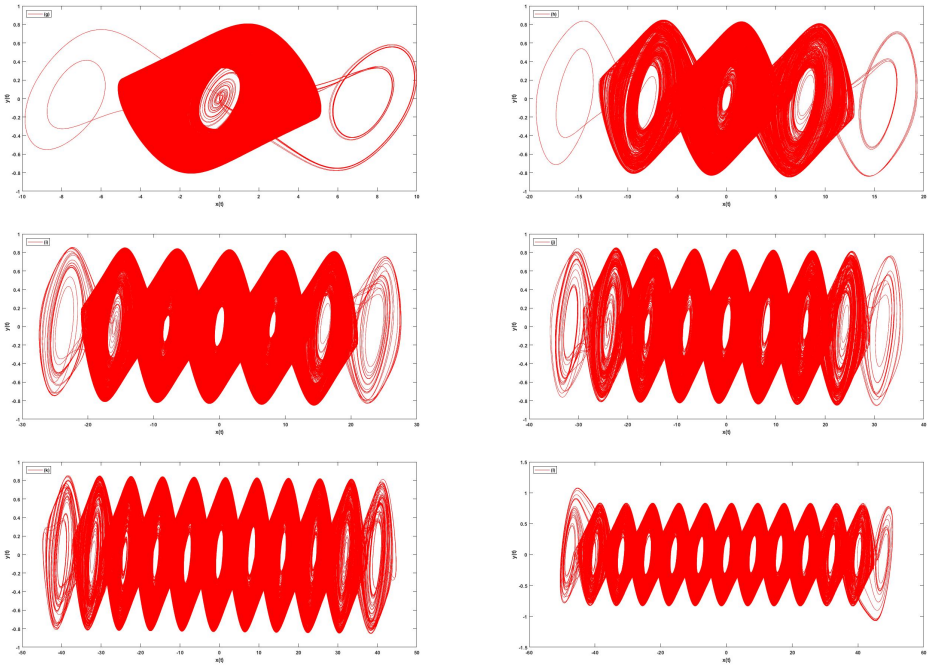

Figure 16: (Continued of **Fig. ??**). Phase portrait of Chua system for different values ε and $c = 21$(attractors). (g) 3-spirals for $\varepsilon = 0.86$, (h) 5-spirals for $\varepsilon = 0.978$, (i) 7-spirals for $\varepsilon = 0.989$, (j) 9-spirals for $\varepsilon = 0.993$, (k) 11-spirals for $\varepsilon = 0.9953$, (l) 13-spirals for $\varepsilon = 0.9994$

Remark 2.

1/ These results (all figures) are obtained by integrating the differential equation, using the Matlab program over a sufficient period of time.

2/ When we increase the value of ε, the number of scrolls keeps increasing with staying in the chaos zone.

3/ We have two different notions of bifurcation, the first one the classic definition, the second definition by Menacer et al.

6 Conclusion

In this article hidden bifurcations of the multispiral Chua Chaotic attractor generated by sine function have been considered. The general shape of the chaotic attractors have been described in terms of the number of spirals (also denoted multiscroll attractor) governed by an integer parameter c. Due to the integer nature of this parameter it is not possible to observe bifurcations from n to $n+2$ spirals when this parameter is increased by one. However, using the method of hidden bifurcations, an additional real parameter ε was introduced in order to observe such bifurcations. The highlighted routes of bifurcation found numerically display chaotic attractors with either an even number or an odd number of spirals. Moreover, this hidden parameter allowed to find bifurcation of the multispiral Chua attractor from a stable state to a chaotic state. Furthermore, the Routh-Hurwitz criteria was used to study the stability of the original equilibrium point of the Chua attractor.

Appendix A: Analytical-Numerical Method for Searching Hidden Attractor Localization

Leonov [15] and Leonov et al. [14], [16] suggested the method for searching attractors of multidimensional nonlinear dynamical systems with scalar nonlinearity.

Their method is based on numerical continuation: a sequence of linked systems is constructed such that for the first (starting) system the initial data for numerical computation of possible oscillating solution (starting oscillation) can be obtained analytically and the transformation of this starting solution oscillation when is passing from one system to another is followed numerically. This suggested approach is generalized in [12], [11], [13] to the system of the form

$$\dot{U} = MU + qH(r^T U), \quad U \in \mathbb{R}^n \tag{17}$$

where M is a constant $n \times n$-matrix, $H(\sigma)$ is a continuous piecewise differentiable function satisfying the condition $H(0) = 0$, q, r are constant $n-$dimensional vectors and ^{T} denote transpose operation.

We present here their method in the simplified case $n = 3$. Therefore we consider the equation

$$\dot{U} = MU + qH(r^T U), \quad U \in \mathbb{R}^3 \tag{18}$$

where $H(\sigma)$ is a continuous nonlinear function.

They then define a coefficient of harmonic linearization χ (suppose that such χ exists) in such a way that the matrix

$$M_0 = M + \chi q r^T \tag{19}$$

of the linear system

$$\dot{U} = MU \tag{20}$$

has a pair of purely imaginary eigenvalues $\pm i\omega_0, (\omega_0 > 0)$ and the other eigenvalue has negative real part. In practice, to determine χ and ω_0 they use the transfer function $W(m)$ of system(17)

$$W(m) = r(M - mI)^{-1} q \tag{21}$$

where m is a complex variable and I is a unit matrix. The number $\omega_0 > 0$ is determined from the equation $\operatorname{Im} W(i\omega_0) = 0$ and χ is calculated by the formula $\chi = -\operatorname{Re} W(i\omega_0)^{-1}$.

Therefore, system (17) can rewriten as

$$\dot{U} = M_0 U + qg(r^T U), \quad U \in \mathbb{R}^3 \tag{22}$$

where $g(\sigma) = H(\sigma) - \chi\sigma$.

Following that, they introduce a finite sequence of continous functions $g^0(\tau)$, $g^1(\tau), ..., g^m(\tau)$ in such a way that the graphs of neighboring functions $g^j(\tau)$ and $g^{j+1}(\tau)$, $(j = 0, ..., m-1)$ in a sense, slightly differ from each other, the function $g^0(\tau)$ is small and $g^m(\tau) = g(\tau)$. The smallness of function $g^0(\tau)$, allows to apply the method of harmonic linearization (describing function method) to the system

$$\dot{U} = M_0 U + qg^0(r^T U), \quad U \in \mathbb{R}^3 \tag{23}$$

if the stable periodic solution $U^0(t)$ close to harmonic one is determined. Then for the localization of an attractor of the original system (22), one can follow numerically the transformation of this periodic solution (a starting oscillating is an attractor, not including equilibria, denoted further by A_0) simply increasing j.

By nonsingular linear transformation S $(U = SZ)$ the system (23) can be reduced to the form

$$\begin{cases} \dot{z}_1(t) &= -\omega_0 z_2(t) + b_1 g^0(z_1(t) + c_3^T z_3(t)) \\ \dot{z}_2(t) &= \omega_0 z_1(t) + b_2 g^0(z_1(t) + c_3^T z_3(t)) \\ \dot{z}_3(t) &= a_3 z_3(t) + b_3 g^0(z_1(t) + c_3^T z_3(t)) \end{cases} \tag{24}$$

where $z_1(t)$, $z_2(t)$, $z_3(t)$ are scalar values, a_3, b_1, b_2, b_3, c_3 are real numbers and $a_3 < 0$.

The describing function G is defined as

$$G(\tau) = \int_0^{\frac{2\pi}{\omega_0}} g(\cos(\omega_0 t)\tau)\cos(\omega_0 \tau)dt. \tag{25}$$

Theorem. *[14] If it can be found a positive τ_0 such that*

$$G(\tau_0) = 0, \qquad b_1 \frac{dG(\tau)}{d\tau} \mid_{\tau=\tau_0} < 0.$$

has a stable periodic solution with initial data $U^0(0) = S(z_1(0), z_2(0), z_3(0))^T$ at the initial step of algorithm one has $z_1(0) = \tau_0 + O(\varepsilon)$, $z_2(0) = 0$, $z_3(0) = O_{n-2}(\varepsilon)$, where $O_{n-2}(\varepsilon)$ is an $(n-2)$-dimensional vector such that all it's components are $O(\varepsilon)$.

References

[1] Ahmed, E., El-Sayed, A., and El-Saka, H. A. On some routh–hurwitz conditions for fractional order differential equations and their applications in lorenz, rössler, chua and chen systems. *Physics Letters A 358*, 1 (2006), 1–4.

[2] Arena, P., et al. Generation of n-double scrolls via cellular neural networks. *International Journal of circuit theory and applications 24*, 3 (1996), 241–252.

[3] Boughaba, S., and Lozi, R. Fitting trapping regions for chua's attractor—a novel method based on isochronic lines. *International Journal of Bifurcation and Chaos (IJBC) 10*, 01 (2000), 205–225.

[4] CHUA, L. The genesis of chua's circuit. *Archiv fur Elektronik und Ubertragungstechnic 46* (1992), 250–257.

[5] Chua, L., Komuro, M., and Matsumoto, T. The double scroll family. *IEEE transactions on circuits and systems 33*, 11 (1986), 1072–1118.

[6] Circuit, M. R. C. A paradigm for chaos, 1993.

[7] Duan, Z., Wang, J., and Huang, L. Multi-input and multi-output nonlinear systems: Interconnected chua's circuits. *IJBC 14*, 09 (2004), 3065–3081.

[8] Hirsch, M. W., Smale, S., and Devaney, R. L. *Differential Equations, Dynamical Systems, and an Introduction to Chaos*, vol. 60. Elsevier, 2003.

[9] Huang, A., Pivka, L., Wu, C. W., and Franz, M. Chua's equation with cubic nonlinearity. *IJBC 6*, 12a (1996), 2175–2222.

[10] Khibnik, A. I., Roose, D., and Chua, L. O. On periodic orbits and homoclinic bifurcations in chua's circuit with a smooth nonlinearity. *IJBC 3*, 02 (1993), 363–384.

[11] Leonov, G., and Kuznetsov, N. Analytical-numerical methods for investigation of hidden oscillations in nonlinear control systems. *IFAC Proceedings Volumes 44*, 1 (2011), 2494–2505.

[12] Leonov, G., Kuznetsov, N., and Vagaitsev, V. Localization of hidden chua's attractors. *Physics Letters A 375*, 23 (2011), 2230–2233.

[13] Leonov, G., Kuznetsov, N., and Vagaitsev, V. Hidden attractor in smooth chua systems. *Physica D: Nonlinear Phenomena 241*, 18 (2012), 1482–1486.

[14] Leonov, G., Vagaitsev, V., and Kuznetsov, N. Algorithm for localizing chua attractors based on the harmonic linearization method. In *Doklady Mathematics* (2010), vol. 82, Springer, pp. 663–666.

[15] Leonov, G. A. On the method of harmonic linearization. *Automation and Remote Control 70*, 5 (2009), 800–810.

[16] Leonov, G. A., and Kuznetsov, N. V. Hidden attractors in dynamical systems. from hidden oscillations in hilbert–kolmogorov, aizerman, and kalman problems to hidden chaotic attractor in chua circuits. *IJBC 23*, 01 (2013), 1330002.

[17] Lorenz, E. N. Deterministic nonperiodic flow. *Journal of atmospheric sciences 20*, 2 (1963), 130–141.

[18] Lozi, R. A computing method for bifurcation boughs of nonlinear eigenvalue problems. *Bulletin of the American Mathematical Society 81*, 6 (1975), 1127–1129.

[19] Lozi, R., and Ushiki, S. The theory of confinors in chua's circuit: accurate analysis of bifurcations and attractors. *IJBC 3*, 02 (1993), 333–361.

[20] Lur'e, A. *Certain Nonlinear Problems in the Theory of Automatic Control, Gostekhizat, Moscow, Leningrad*. 1951.

[21] Marsden, J., and McCracken, M. The hopf bifurcation and its applications, 1976.

[22] Matsumoto, T. A chaotic attractor from chua's circuit. *IEEE Transactions on Circuits and Systems 31*, 12 (1984), 1055–1058.

[23] Menacer, T., Lozi, R., and Chua, L. O. Hidden bifurcations in the multispiral chua attractor. *IJBC 26*, 14 (2016), 1630039.

[24] Poincaré, H. Sur l'équilibre d'une masse fluide animée d'un mouvement de rotation. *Bulletin astronomique, Observatoire de Paris 2*, 1 (1885), 109–118.

[25] Sattinger, D. Topics in stability and bifurcation theory lecture notes in mathematics 309 springer-verlag, 1973.

[26] SHIL'NIKOV, L. P. Chua's circuit: Rigorous results and future problems. *IJBC 4*, 03 (1994), 489–519.

[27] Suykens, J., Huang, A., and Chua, L. A family of n-scroll attractors from a generalized chua's circuit. *AEU-Archiv für Elektronik und Übertragungstechnik 51*, 3 (1997), 131–138.

[28] Suykens, J., and Vandewalle, J. Quasilinear approach to nonlinear systems and the design of n-double scroll (n= 1, 2, 3, 4,. . .). *IEE Proceedings G (Circuits, Devices and Systems) 138*, 5 (1991), 595–603.

[29] Tang, W. K., et al. Generation of n-scroll attractors via sine function. *IEEE Transactions on Circuits and Systems I: Fundamental Theory and Applications 48*, 11 (2001), 1369–1372.

[30] Yalcin, M., Suykens, J., and Vandewalle, J. Experimental confirmation of 3-and 5-scroll attractors from a generalized chua's circuit. *IEEE Transactions on Circuits and Systems I: Fundamental Theory and Applications 47*, 3 (2000), 425–429.

[31] Zhong, G.-Q., and Ayrom, F. Experimental confirmation of chaos from chua's circuit. *International journal of circuit theory and applications 13*, 1 (1985), 93–98.